

Damage Identification Technique based on the Spectral Element Method using High-Frequency Excitation

T. Matsuo, A. Furukawa & K. Nishikawa
Graduate School of Engineering, Kyoto University, Kyoto



SUMMARY:

A damage identification technique using high-frequency excitation based on the spectral element method is presented. Considering a drawback of the low-frequency-based damage identification technique, this study proposes a damage identification technique using kHz-level frequency that can detect smaller damage efficiently. It is assumed that a structure is excited with a harmonic force by a piezoelectric actuator and that the method focuses on the difference of the frequency response function by damage. Moreover, it uses the spectral element method that is suitable for analyzing structural responses at high frequency domain. The effectiveness of the proposed method was verified by numerical simulations using a steel truss bridge.

Keywords: damage identification, spectral element method, high-frequency, frequency response function

1. BACKGROUND AND OBJECTIVE

Japan is one of the most earthquake-prone countries of the world, and aged infrastructures are in danger of getting serious damages during earthquakes. In order to prevent these damages, structural condition has to be checked on regular basis and their maintenance has to be done properly. Also, the judgment of the degree of structural damage after major earthquakes is currently relying on visual inspection. Visual inspection takes a lot of time and efforts, and in addition, it has problems such as oversight and labor shortage, so it is desirable to make a diagnosis more conveniently and economically. Therefore, it is necessary to develop a reliable method for damage identification.

Among previous damage identification techniques, the methods using Hz-level frequency such as ambient vibration observation have a difficulty in detecting small damage, and the methods using MHz-level frequency such as ultrasonic detection can only examine very small area at a time, therefore it takes a lot of time to scan the entire structure. With this background, this study proposes a damage identification technique using kHz-level frequency that can detect small damage efficiently. It is assumed that the structure is excited with harmonic force by the piezoelectric actuator, and that the method focuses on the difference of the frequency response function (FRF) by damage. Moreover, it uses the spectral element method, which is suitable for analyzing high-frequency domain. The effectiveness of the proposed method was verified by numerical simulations.

2. THE SPECTRAL ELEMENT METHOD

The spectral element method is the frequency domain method to build dynamic element stiffness matrices for each frequency. This section provides to derive element matrices for Euler-Bernoulli beam.

2.1. Vibration in the axial direction

In the axial direction, the equation of motion is represented by

$$EA \frac{\partial^2 u(x, t)}{\partial x^2} - \rho A \frac{\partial^2 u(x, t)}{\partial t^2} = 0 \quad (2.1)$$

where $u(x, t)$ is the axial displacement, E is the Young's modulus, A is the cross-sectional area, ρ is the mass density, t is the time, and x is the position. When $U(x, \omega)$ is the Fourier transformation of $u(x, t)$, the equation of motion at frequency domain is represented by

$$EA \frac{d^2 U(x, \omega)}{dx^2} + \omega^2 \rho A U(x, \omega) = 0 \quad (2.2)$$

where ω is the angular frequency. This solution is estimated by the following equation.

$$U(x, \omega) = a e^{-ik_L x} \quad (2.3)$$

By substituting Eqn. 2.3 into Eqn. 2.2,

$$k_L = \sqrt{\frac{\rho}{E}} \quad (2.4)$$

For a finite rod element of length l , $U(x, \omega)$ is expressed as follows.

$$U(x, \omega) = a_1 e^{-ik_L x} + a_2 e^{+ik_L x} = \mathbf{e}(x, \omega) \mathbf{a} \quad (2.5)$$

where

$$\begin{aligned} \mathbf{e}(x, \omega) &= [e^{-ik_L x} \quad e^{+ik_L x}] \\ \mathbf{a} &= \{a_1 \quad a_2\}^T \end{aligned} \quad (2.6)$$

From the boundary condition of the element,

$$\mathbf{d}(\omega) = \begin{Bmatrix} U_1 \\ U_2 \end{Bmatrix} = \begin{Bmatrix} U(0) \\ U(l) \end{Bmatrix} \quad (2.7)$$

Substituting Eqn. 2.5 into Eqn. 2.7 gives

$$\mathbf{d}(\omega) = \begin{bmatrix} \mathbf{e}(0, \omega) \\ \mathbf{e}(l, \omega) \end{bmatrix} \mathbf{a} = \begin{bmatrix} 1 & 1 \\ e^{-ik_L l} & e^{+ik_L l} \end{bmatrix} \mathbf{a} \quad (2.8)$$

By eliminating \mathbf{a} from Eqn. 2.5 by using Eqn. 2.8, the following equation is obtained.

$$U(x, \omega) = \mathbf{N}_R(x, \omega) \mathbf{d}(\omega) \quad (2.9)$$

where

$$\begin{aligned} \mathbf{N}_R(x, \omega) &= \mathbf{e}(x, \omega) \begin{bmatrix} 1 & 1 \\ e^{-ik_L l} & e^{+ik_L l} \end{bmatrix}^{-1} = [N_{R1}(x, \omega) \quad N_{R2}(x, \omega)] \\ N_{R1}(x, \omega) &= \sin[k_L(l-x)] / \sin(k_L l) \\ N_{R2}(x, \omega) &= \sin(k_L x) / \sin(k_L l) \end{aligned} \quad (2.10)$$

The axial force at frequency domain is represented by

$$N(x, \omega) = EA \frac{dU(x, \omega)}{dx} \quad (2.11)$$

The relationship between axial force and nodal point in this element is expressed as follows.

$$\mathbf{f}_c(\omega) = \begin{Bmatrix} N_1 \\ N_2 \end{Bmatrix} = \begin{Bmatrix} -N(0) \\ +N(l) \end{Bmatrix} \quad (2.12)$$

Substituting Eqn. 2.9 and Eqn. 2.11 into the right-hand side of Eqn. 2.12 gives

$$\mathbf{S}_R(\omega)\mathbf{d}(\omega) = \mathbf{f}_c(\omega) \quad (2.13)$$

The dynamic stiffness matrix $\mathbf{S}_R(\omega)$ is derived as follows.

$$\mathbf{S}_R(\omega) = \frac{EA}{l} \begin{bmatrix} \frac{k_L l}{\tan k_L l} & -\frac{k_L l}{\sin k_L l} \\ -\frac{k_L l}{\sin k_L l} & \frac{k_L l}{\tan k_L l} \end{bmatrix} \quad (2.14)$$

2.2. Vibration in the shear/bending direction

The equation of motion in the transverse direction is represented by

$$EI \frac{\partial^4 v(x, t)}{\partial x^4} - \rho A \frac{\partial^2 v(x, t)}{\partial t^2} = 0 \quad (2.15)$$

where $v(x, t)$ is the transverse displacement. $V(x, \omega)$, Fourier transformation of $v(x, t)$ is

$$V(x, \omega) = a_1 e^{-ik_F x} + a_2 e^{-k_F x} + a_3 e^{+ik_F x} + a_4 e^{+k_F x} \quad (2.16)$$

where k_F is function of ω

$$k_F = \sqrt{\omega} \sqrt[4]{\frac{\rho A}{EI}} \quad (2.17)$$

From these equations, the dynamic stiffness matrix $\mathbf{S}_B(\omega)$ in the shear/bending direction is derived. In the spectral element method, the influence of mass is included in the dynamic stiffness matrix. Therefore, the future subject is said to be how to take into account the damping.

2.3. Comparison of the spectral element method and the finite element method

It is examined how the element division affects the analytical result of the spectral element method (SEM) and the finite element method (FEM). Target structure is a beam clamped at both ends, and $l=7.38[\text{m}]$, $\rho=7800[\text{kg}/\text{m}^3]$, $E=2.20 \times 10^{11}[\text{N}/\text{m}^2]$, $A=5.50 \times 10^{-3}[\text{m}^2]$ and $I=5.11 \times 10^{-5}[\text{m}^4]$, respectively. The beam is excited by a harmonic force at the center of the beam in the perpendicular direction, and the frequency response function is measured at the center of the beam.

The analytical result is shown in Fig. 2.1. Fig. 2.1(a) is the result of the FEM and Fig. 2.1(b) is the result of the SEM. The horizontal axis is the excitation frequency and the vertical axis is the frequency response function (FRF) obtained by the respective methods. The legend is the number of element

divisions. In the results of the FEM, the FRF differs largely depending on the element divisions, especially at higher frequency. On the other hand, in the results of the SEM, the FRF is independent of element divisions and frequency. From this comparison, the spectral element method is shown to be more valid for the analysis at high frequency.

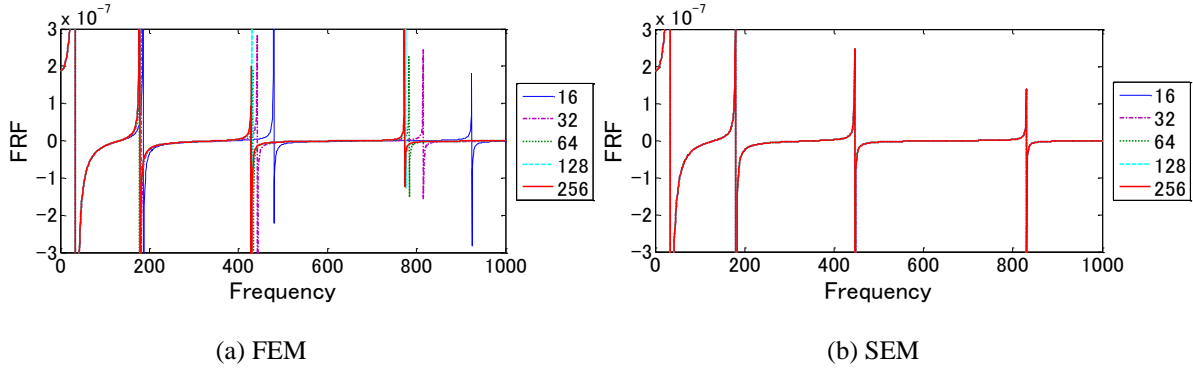


Figure 2.1. Comparison of solutions of FRF and SEM for various element divisions

In the spectral element method, element division is not necessary except for the point where the cross-sectional characteristics change. Therefore, it can save the computational time compared to the finite element method, and is particularly advantageous for high-frequency domain. The damage identification technique proposed in the next section utilizes the frequency response function at the single excitation frequency, which fits well with the characteristics of the spectral element method building dynamic stiffness matrices for each frequency.

3. THE DAMAGE IDENTIFICATION TECHNIQUE

3.1. Damage model

The structural damage is evaluated as reduction of cross-sectional area and reduction of second moment of area. Thus, it is possible to take into account the mass change due to partial loss of area. Also, this paper is intended for non-damped system and damping is not considered. Dynamic stiffness matrix of the entire structure can be modeled as the following equation as a collection of dynamic stiffness matrices of each element.

$$\mathbf{S}(\omega) = \sum_{e=1}^n \mathbf{S}^e(\omega) \quad (3.1)$$

where n is the total number of beam element and $\mathbf{S}^e(\omega)$ is the dynamic stiffness matrix of the e th beam element. When the cross-sectional area and the second moment of area of the e th beam element decrease to δA_e and δI_e , the reduction of the dynamic stiffness matrix of the e th beam element, $\delta \mathbf{S}^e(\omega)$ is represented by

$$\delta \mathbf{S}^e(\omega) = \delta A_e \mathbf{K}_A^e(\omega) + \delta I_e \mathbf{K}_I^e(\omega) \quad (3.2)$$

where

$$\mathbf{K}_A^e(\omega) = \frac{\delta \mathbf{S}^e(\omega)}{\delta A_e}, \quad \mathbf{K}_I^e(\omega) = \frac{\delta \mathbf{S}^e(\omega)}{\delta I_e} \quad (3.3)$$

Thus, the decrement of the dynamic stiffness matrix of entire structure is expressed as follows.

$$\delta\mathbf{S}(\omega) = \sum_{e=1}^n \delta A_e \mathbf{K}_A^e(\omega) + \sum_{e=1}^n \delta I_e \mathbf{K}_I^e(\omega) \quad (3.4)$$

3.2. The response in intact condition

The equation of motion at frequency domain before damage is represented by

$$\mathbf{S}(\omega)\mathbf{X}(\omega) = \mathbf{F}(\omega) \quad (3.5)$$

where is $\mathbf{S}(\omega)$ dynamic stiffness, $\mathbf{X}(\omega)$ is Fourier amplitudes of displacement and $\mathbf{F}(\omega)$ is Fourier amplitudes of external force. The displacement response, $\mathbf{X}(\omega)$ is expressed as follows.

$$\mathbf{X}(\omega) = \mathbf{H}(\omega)\mathbf{F}(\omega) \quad (3.6)$$

$\mathbf{H}(\omega)$ is the inverse matrix of $\mathbf{S}(\omega)$ and indicates frequency response function.

3.3. The response in damaged condition

The equation of motion after damage is represented by

$$(\mathbf{S}(\omega) - \delta\mathbf{S}(\omega))(\mathbf{X}(\omega) + \delta\mathbf{X}(\omega)) = \mathbf{F}(\omega) \quad (3.7)$$

where $\delta\mathbf{X}(\omega)$ is increment of displacement. Substituting Eqn. 3.7 into Eqn. 3.5 and Eqn. 3.4 gives

$$\delta\mathbf{X}(\omega) = \mathbf{H}_d(\omega)\delta\mathbf{S}(\omega)\mathbf{H}(\omega)\mathbf{F}(\omega) \quad (3.8)$$

where $\mathbf{H}_d(\omega)$ is the frequency response function after damage.

$$\mathbf{H}_d(\omega) = [\mathbf{S}(\omega) - \delta\mathbf{S}(\omega)]^{-1} \quad (3.9)$$

By adding the increment of displacement $\delta\mathbf{X}(\omega)$ to the displacement before damage $\mathbf{X}(\omega)$, the displacement after damage $\mathbf{X}'(\omega)$ is obtained.

$$\mathbf{X}'(\omega) = \mathbf{H}(\omega)\mathbf{F}(\omega) + \sum_{e=1}^n \mathbf{U}_A^e(\omega)\mathbf{F}(\omega)\delta A_e + \sum_{e=1}^n \mathbf{U}_I^e(\omega)\mathbf{F}(\omega)\delta I_e \quad (3.10)$$

where

$$\mathbf{U}_A^e(\omega) = \mathbf{H}_d(\omega)\mathbf{K}_A^e(\omega)\mathbf{H}(\omega) \quad , \quad \mathbf{U}_I^e(\omega) = \mathbf{H}_d(\omega)\mathbf{K}_I^e(\omega)\mathbf{H}(\omega) \quad (3.11)$$

3.4. Construction of damage identification equation

Fourier amplitude of acceleration response at excitation frequency divided by the amplitude of the input harmonic external force is considered to be the frequency response function.

$$a(i, j, \omega) = \frac{-\omega^2 \mathbf{X}'(\omega)}{\mathbf{F}(\omega)} = -\omega^2 \left(\mathbf{H}_{ij}(\omega) + \sum_{e=1}^n \mathbf{U}_{Aij}^e(\omega)\delta A_e + \sum_{e=1}^n \mathbf{U}_{Iij}^e(\omega)\delta I_e \right) \quad (3.12)$$

where i is the measurement node, j is the excitation node, ω is the excitation frequency and $a(i, j, \omega)$ are the FRFs at damaged that are measured. $\mathbf{H}_{ij}(\omega)$ are the FRFs at intact and are known value. On the other hand, $\mathbf{U}_{Aij}^e(\omega)$ and $\mathbf{U}_{Iij}^e(\omega)$ are obtained by the structural data at intact, the

excitation frequency and unknown parameters δA_e and δI_e . About Eqn. 3.12, transposing the known terms to the left-hand side and transposing the unknown terms to the right-hand side gives

$$-\omega^2 \sum_{e=1}^n \mathbf{U}_{Aij}^e(\omega) \delta A_e - \omega^2 \sum_{e=1}^n \mathbf{U}_{Iij}^e(\omega) \delta I_e = a(i, j, \omega) + \omega^2 \mathbf{H}_{ij}(\omega) \quad (3.13)$$

This equation is satisfied by each combination of measurement nodes i , excitation nodes j and excitation frequencies ω . By changing the combinations of i , j , ω , and measuring m times, the following simultaneous equation is led.

$$[\mathbf{X}(\delta \mathbf{A}, \delta \mathbf{I})] \{\mathbf{a}\} = \{\mathbf{y}\} \quad (3.14)$$

where

$$\begin{aligned} \mathbf{X}_{l,e}(\delta \mathbf{A}, \delta \mathbf{I}) &= -\omega^2 \mathbf{U}_{Aij}^e(\omega) , \quad \mathbf{X}_{l,n+e}(\delta \mathbf{A}, \delta \mathbf{I}) = -\omega^2 \mathbf{U}_{Iij}^e(\omega) \\ \{\mathbf{a}\} &= \{\delta A_1, \dots, \delta A_n, \delta I_1, \dots, \delta I_n\}^T , \quad \{\mathbf{y}\} = a(i, j, \omega) + \omega^2 \mathbf{H}_{ij}(\omega) \end{aligned} \quad (3.15)$$

$l(l = 1, \dots, m)$ is the measurement number. Eqn. 3.14 is simultaneous equations of m included in unknown values of $2n$ and is called damage identification equation. Solving this equation, damage location and damage degree are detected.

4. ANALYTICAL MODEL

4.1. Target structure

Numerical simulations are performed for steel truss bridge. Target structure is the single-span steel truss bridge length 47.0m, width 4.8m, and the material properties are shown in Table 4.1. The boundary condition in the ends of diagonal member is modelled by fixed condition. The three-dimensional structural influence is ignored, so the truss is modelled by two-dimensional beam element. The sixth diagonal member from the left in Fig. 4.1 is a target member. The truss is divided by elements as shown in Fig. 4.1. The bottom 1/4 of the target member is divided finely as shown in Fig. 4.2 because these nodes are measurement nodes. The upper 3/4 is divided at the center into two parts because this node is excitation node.

4.2. Damage model

The corrosion damage whose length is 16cm and thickness is 3mm at 58cm from the bottom is assumed as shown in Fig. 4.2. The reduction rates in cross-sectional area A and second moment of area I of the damage element (element No. 35) are 0.09 and 0.15, respectively.

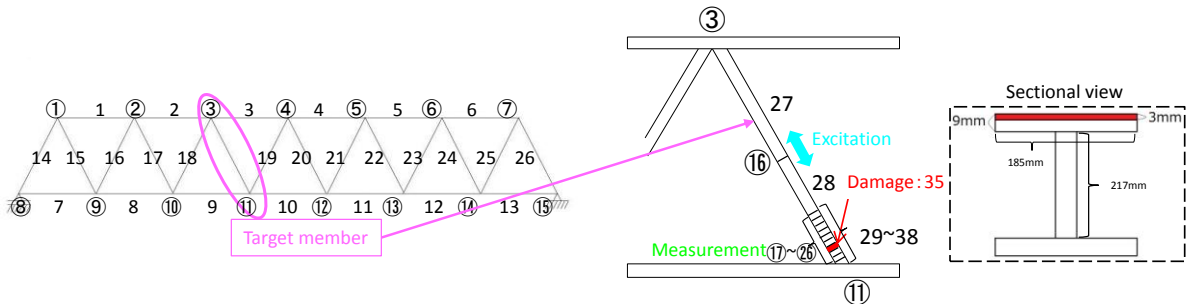


Figure 4.1. Analytical model

Figure 4.2. Damage model

Table 4.1. Material properties

	Upper member	Diagonal member	Bottom member	Floor
Unit weight (kg/m ³)	7800	7800	7800	2500
Young's modulus (N/m ²)	2.20×10^{11}	2.20×10^{11}	2.20×10^{11}	2.50×10^{10}
Cross-sectional area(m ²)	1.21×10^{-2}	5.50×10^{-3}	9.40×10^{-3}	1.00
Second moment of area(m ⁴)	1.21×10^{-4}	5.11×10^{-5}	6.21×10^{-5}	1.33×10^{-2}
Damping ratio	0	0	0	0

5. CHANGES IN THE VIBRATION CHARACTERISTICS DUE TO DAMAGE

5.1. Deformation of the truss

The excitation node and excitation frequency are fixed and the frequency response functions are measured at all nodes. Therefore, the deformed shape of the truss bridge can be shown for various frequencies. The truss is excited at 1Hz or 5000Hz in the axial direction. The frequency 5000Hz is close to the resonance frequency 6000Hz of the piezoelectric actuator which is assumed to use.

The result at 1Hz is shown in Fig. 5.1 and that at 5000Hz is shown in Fig. 5.2. It is found that whole truss is vibrated at 1Hz. On the other hand, it is found that the only excited member is vibrated locally and the higher order mode can be observed at 5000Hz. Note that the target member is divided into 132 and other members are divided into two because the response can be obtained.

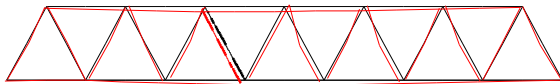


Figure 5.1. The deformed shape at 1Hz

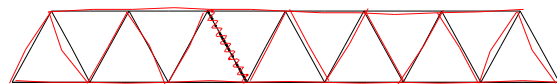


Figure 5.2. The deformed shape at 5000Hz

5.2. Changes in the frequency response function due to damage

It is investigated how the frequency response function of target member changes due to damage. Target member is divided into 132 elements. By exciting at the center of the target member, the FRFs of all nodes are measured. It is excited at 1Hz or 5000Hz in the axial direction.

The result at 1Hz is shown in Fig. 5.3 and that at 5000Hz is shown in Fig. 5.4. The vertical axis is FRF and the horizontal axis is the measurement number. Measurement No.1 and No.133 are located on top and the bottom of the target member, respectively. At 1Hz, there is little FRF difference due to damage. On the other hand, at 5000Hz, higher-order mode is shown, and the difference of FRF is larger. It can be confirmed that high-frequency is more sensitive for damage.

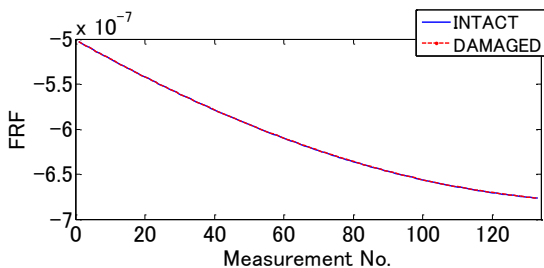


Figure 5.3. FRF at 1Hz

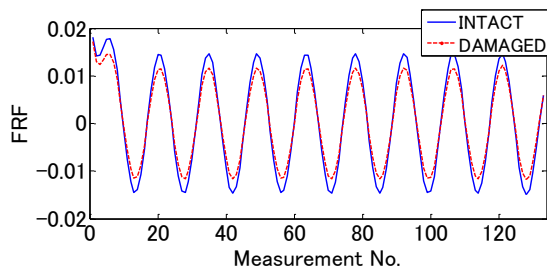


Figure 5.4. FRF at 5000Hz

6. THE DAMAGE IDENTIFICATION ANALYSIS

6.1. Analytical case

6.1.1. Case A

The damage identification analysis for steel truss bridge is conducted with using the method proposed at section 3. The element division and damage model were shown in section 4. The damage, that is assumed to be located at element No. 35 with the reduction of 9% cross-sectional area and 15% second moment of area, is an aim to be detected. The truss is excited at the center of the target member and is measured at the bottom 1/4 part of the target member (measurement nodes No.: 17~26). The excitation and measurement is in the axial or transverse direction and the excitation frequency is 1Hz or 5000Hz, respectively. 1% measurement noise is considered.

6.1.2. Case B

It is investigated if a member except target member is damaged, how it influences result. The damage at an upper member (element No. 3) next to target member is assumed. Cross-sectional area and second moment of area at the upper member is decreased sufficiently by half to see the effect of the damage at the upper member on the damage identification results of the target member. The excitation node is the center of the target member and the measurement nodes are same to Case A. The truss is excited at 1Hz or 5000Hz in the axial direction.

6.2. Analytical result

6.2.1. Case A

The results at 1Hz are shown in Figs. 6.1 and 6.3. The results at 5000Hz are shown in Figs. 6.2 and 6.4. Also, Figs. 6.1 and 6.2 show the results in the axial direction and Figs. 6.3 and 6.4 show the results in the transverse direction. In each figure, (a) is the results of cross-sectional area and (b) is those of second moment of area. The vertical axis is the identified reduction rate, and the horizontal axis is the element number of the target member (element No. 27-38).

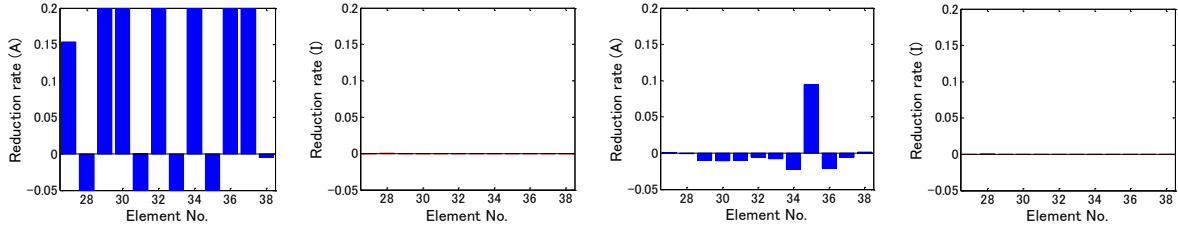
At first, when it is excited in the axial direction, it was impossible to detect 9% reduction of cross-sectional area of element No. 35 at 1Hz, but was possible at 5000Hz. At 1Hz, 1% measurement noise couldn't be ignored and false detection occurred. On the other hand, at 5000Hz, the noise didn't influence the results and the assumed damage could be detected. Moreover, it could be detected both at 1Hz and 5000Hz without measurement noise, so it is said that higher-frequency is resistant to noise.

Next, it found that when it is excited and measured in the axial direction, the accuracy of detection of cross-sectional area is higher. On the other hand, when it is excited and measured in the transverse direction, the accuracy of detection of second moment of area is higher. Also, at 5000Hz, the accuracy of detection of cross-sectional area in the axial direction is higher than that of second moment of area in the transverse direction. This is because excitation frequency 5000Hz is close to natural frequency dominated in the axial direction and more sensitive data of reduction of cross-sectional area can be obtained. Because the gradient of FRF is sharp near natural frequency, it is said that the FRF at such a frequency changes larger even if the natural frequency changes a little due to damage.

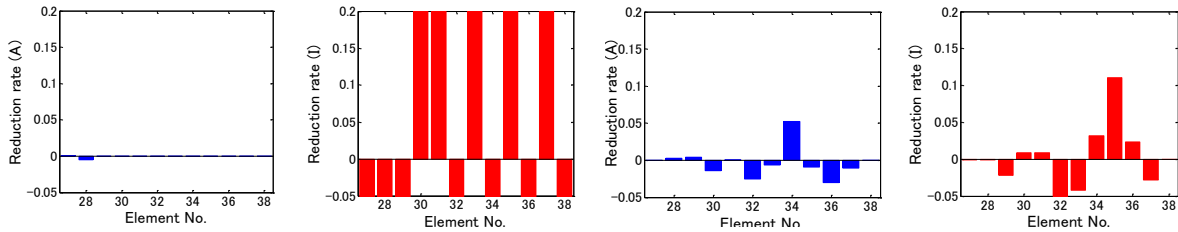
6.2.2. Case B

The result at 1Hz is shown in Fig. 6.5 and that at 5000Hz is shown in Fig. 6.6. The horizontal axis is element number. Element No. 27-38 are target member and element No. 1-26 are the other members. The vertical axis is reduction rate of cross-sectional area.

At 1Hz, false detection occurred. On the other hand, at 5000Hz, reduction of cross-sectional area of element No. 35 can be detected without the influence from other members. Looking at the result at 1Hz, the damage of element No. 35 could be detected more accurately than case A because it was not considered measurement noise. At higher-frequency, target member can be only excited and influence of other members can be removed.



(a) Cross-sectional area (b) Second moment of area **Figure 6.1.** Excited at 1Hz in axial dir., Case A (a) Cross-sectional area (b) Second moment of area **Figure 6.2.** Excited at 5000Hz in axial dir., Case A



(a) Cross-sectional area (b) Second moment of area **Figure 6.3.** Excited at 1Hz in transverse dir., Case A (a) Cross-sectional area (b) Second moment of area **Figure 6.4.** Excited at 5000Hz in transverse dir., Case A

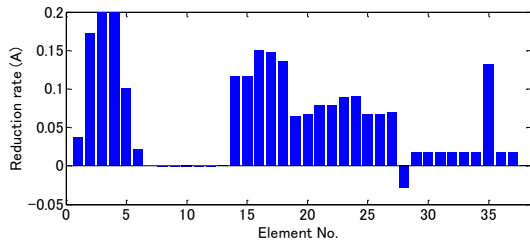


Figure 6.5. Excited at 1Hz, Case B

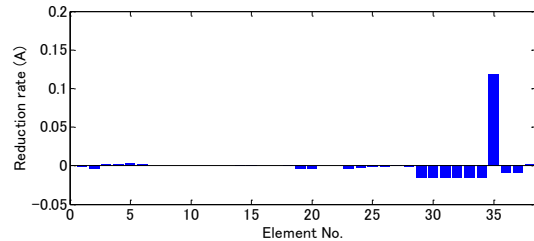


Figure 6.6. Excited at 5000Hz, Case B

7. THE DAMAGE IDENTIFICATION USING THE GROUPING METHOD

In this section, it is verified whether the damage can be detected efficiently by using the grouping method. In this method, all elements are divided into some groups and elements of same group are assumed to be same damage. Therefore, the number of parameters to identify is decreased and the elements which are estimated at no-damage are removed. By using this method the measurement number can be decreased.

The analysis is conducted for the steel truss bridge from the section 4. The truss is excited at the center of the target member in the axial direction by 5000Hz. The measurement nodes are 4 nodes; 17, 20, 23 and 26. The measurement noise 1% is considered. The elements are divided into 4 groups because the measurement number is 4. The elements except target member are assumed to be undamaged, so they are excluded from analytical target. Note that the damage is detected as the reduction of cross-sectional area because it is excited in the axial direction.

At Step 1, the 12 elements of target member were divided into 4 groups of 3 elements; element No.

27-29, 30-32, 33-35 and 36-38. The result is shown in Fig. 7.1(a). The fourth group (element No. 36-38) became negative, so it was regarded as no-damage and excluded.

At Step 2, 4 groups (27-28, 29-30, 31-32, 33-35) were made from the 9 elements remained at Step 1. The result is shown in Fig. 7.1(b). Element No. 27 and 28 were excluded.

At Step 3, 4 groups (29, 30-31, 32-33, 34-35) were made from the 7 elements remained at Step 2. The result is shown in Fig. 7.1(c). Element No. 29, 30 and 31 were excluded.

At Step 4, 4 groups (32, 33, 34, 35) were made from the 4 elements remained at Step 3. The result is shown in Fig. 7.1(d). Only 35 was remained and as a result it is found that element No. 35 is damaged.

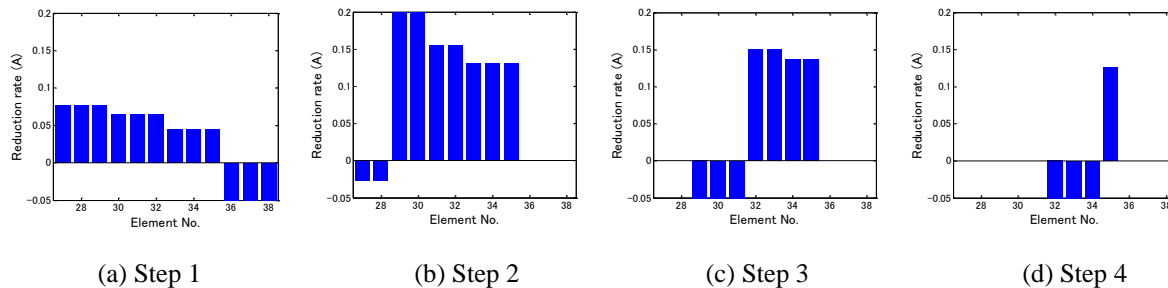


Figure 7.1. Grouping method

8. CONCLUSION

A damage identification technique using high-frequency excitation based on the spectral element method is presented. The effectiveness was verified by numerical simulations for steel truss bridge. It was found that whole truss is vibrated when the target member is excited at 1Hz, but the only excited member is vibrated locally and the higher order mode can be observed when the target member is excited at 5000Hz. By a comparison of the changes of frequency response function, it could be confirmed that high-frequency is more sensitive to damage. According to the analysis, at high-frequency excitation, it was able to detect the damage which cannot be detected at low-frequency excitation. It was also found that the damage can be detected locally by considering single target member when excitation at high-frequency is used. By using the grouping method, the number of measurements could be decreased.

REFERENCES

- Furukawa, A. and Otsuka, H. (2008). Localized Damage Identification Using Fourier Amplitudes at High Frequency. *Journal of Applied Mechanics*. **Vol.11**, 27-37.
- Yoshioka, T., Harada, M., Yamaguchi, H. and Itou, S. (2008). A Study on the Vibration Characteristics Change of the Steel Truss Bridge by the Real Damage of Diagonal Member. *Journal of Structural Engineering*. **Vol.54A**, 199-208.
- Usik L. (2009). Spectral Element Method in Structural Dynamics, John Wiley & Sons (Asia) Pte Ltd
- Furukawa, A., Otsuka, H. and Umebayashi F. (2005). Experimental Study on Changes in Vibrational Characteristics due to Structural Damage. *Journal of Earthquake Engineering*. **Vol.28**, No.19.
- Yoshioka, T., Yamaguchi, H., Itou, S. and Harada, M. (2009). Identification of Vibration Characteristics of the Steel Truss Bridge and Influence of Diagonal Member Damage on Damping. *Journal of Structural Engineering*. **Vol.55A**, 295-305.